

# Investigation of single-factor calibration of the wave-number scale in Fourier-transform spectroscopy

Marc L. Salit, Craig J. Sansonetti, Damir Veza,\* and John C. Travis

*National Institute of Standards and Technology, Gaithersburg, Maryland 20899*

Received January 6, 2004; revised manuscript received March 22, 2004; accepted March 31, 2004

We have used the fundamental and frequency-doubled output of a single-frequency tunable laser locked to a precisely known transition in molecular iodine to provide calibration of a Fourier-transform spectrometer (FTS) in the visible and near-ultraviolet regions and to investigate the limiting uncertainty involved in calibrating spectra by using a single multiplicative correction to the entire optical frequency scale. An integrating sphere was used to introduce the laser light as a pseudoincoherent source and provide uniform illumination of the FTS field of view. The sphere also served to combine the laser beams with light from a series of mercury electrodeless discharge lamps containing argon carrier gas at selected pressures. Four strong lines in the spectrum of  $^{198}\text{Hg}$  were measured with these lamps to obtain precise wavelengths and argon-pressure-shift coefficients. These lines, emitted from lamps with argon pressures in the range 33 Pa (0.25 Torr) to 1330 Pa (10 Torr), are suitable for future calibration of FT spectra without need for the laser source. The limiting relative uncertainty component in the reported wavelengths is  $6.19 \times 10^{-9}$ , as estimated from observed deviation of the frequency ratios of the calibration lasers from the exact value of 2. The adequacy of a single multiplicative correction factor for the absolute calibration of an individual FT spectrum is supported by our data, at the level of better than a part in  $10^8$ . © 2004 Optical Society of America

*OCIS codes:* 300.6300, 300.6210, 020.3690, 120.3180, 120.6200.

## 1. INTRODUCTION

Although Fourier-transform spectroscopy (FTS) has achieved dominance in the midinfrared domain owing to the multiplex advantage, its most valuable characteristic in the ultraviolet (UV) and visible range is the intrinsic accuracy of its optical frequency axis.<sup>1–6</sup> This accuracy derives from control of the sampling of the interferogram by a single-mode helium–neon laser whose frequency is stabilized to five parts in  $10^9$ . Even so, the intrinsic accuracy of the frequency scale is limited by the degree to which the optical axis of the sample beam is perfectly aligned with the optical axis of the control laser as well as by the finite size of the entrance aperture.<sup>7</sup> Although a “cosine error” of the order of  $10^{-5}$  may be acceptable for many spectroscopic applications, absolute accuracy may in principal be considerably improved by a multiplicative correction of the frequency scale using a single calibration constant. This correction can be written in the form

$$\sigma_{\text{true}} = (1 + k_{\text{eff}})\sigma_{\text{apparent}},$$

where  $\sigma_{\text{true}}$  is the corrected wave number,  $\sigma_{\text{apparent}}$  is the uncorrected wave number, and  $k_{\text{eff}}$  is the correction factor that must be determined based on the measured positions of one or more well-known spectral lines.<sup>7</sup>

The adequacy of a single correction factor to provide an accurate calibration for the frequency scale of an entire spectrum is widely accepted in FTS theory (with proper regard for the potential for line shifts due to field and pressure effects in calibration lines).<sup>7,8</sup> Confidence that a single multiplicative correction can define the wave number at all spectral points to the same relative accuracy,

that of the calibration constant, underlies a principal advantage of the broadband coverage available in FTS. However, in an earlier report,<sup>9</sup> we noted a monotonic change in the apparent calibration constant as a function of the energy of the calibration line used for both mercury and argon discharges. A similar slope observed for argon by Learner and Thorne<sup>7</sup> in their seminal work on FTS calibration was attributed to a pressure difference between the lamps used for the original reference data and the calibration lamp. They noted that the pressure-shift coefficient increased with the energy of the upper state of a transition and restricted the lines used for calibration to the lowest-lying states to achieve the desired accuracy.

We report here the use of a frequency-doubled laser locked to a known spectral line as a definitive calibration source in the visible with a built-in consistency check in the UV, as suggested in the “Note in proof” in our previous work.<sup>9</sup> Consistency is evaluated by the degree to which the laser fundamental and second harmonic yield the same calibration constant, or, equivalently, how precisely the frequency ratio of the measured second-harmonic signal to the measured fundamental signal equals two, as compared with the propagated uncertainty.

The use of an integrating sphere as the effective source for filling the field of view of the FTS was previously proposed as a means of using well-known spectral lines in one source to calibrate measurements made with another source.<sup>9</sup> In the present work, we have used this method to combine the visible and UV laser beams as calibration sources with light emitted by a  $^{198}\text{Hg}$  electrodeless discharge lamp. The sphere permits us to satisfy two calibration recommendations of Learner and Thorne<sup>7</sup>—a

common effective source for the calibrant and measured features, and uniform illumination of the entrance aperture—at the cost of a severe loss in signal strength.<sup>9</sup> This is ideal for introducing the laser signal into the FTS, as attenuation of the laser is necessary and a quasi-pseudoincoherent source results, but it limits the Hg measurements to only the most intense lines. We have measured four lines of <sup>198</sup>Hg in lamps produced with four different Ar carrier gas pressures in order to produce results that can be compared directly with those obtained by Kaufman at the National Bureau of Standards over four decades ago using Fabry–Perot interferometry.<sup>10</sup>

## 2. EXPERIMENT

The essential components of the experiment are illustrated in schematic form in Fig. 1. A 100-mm-diameter integrating sphere was used to couple the nearly collinear fundamental and second-harmonic laser beams into the FTS in such a way as to simulate an incoherent source and fill the field of view of the FTS uniformly. A removable plug in the integrating sphere permitted light from a mercury-discharge lamp to be commingled with the laser light as a common source. Beyond the central role played by the integrating sphere, the principal parts of the experiment were the laser system, the electrodeless-discharge lamp, and the FTS.

### A. Laser System

The laser system was based on a single-frequency cw ring dye laser pumped by an Ar-ion laser. The ring laser, which was equipped with an intracavity frequency doubler, was operated with the dye DCM (4-dicyanmethylene-2-methyl-6-4H-pyran) and produced approximately 300 mW of power in the red fundamental beam and approximately 2 mW in the UV second-harmonic beam. The laser linewidth was approximately 1 MHz at the fundamental frequency. Generation of the UV beam by frequency doubling a cw laser in a nonlinear crystal ensures that the wave numbers of the red and UV beams are related to each other by a factor of exactly 2.

The dye laser was stabilized by locking it to a hyperfine component of molecular iodine. The iodine spectrum was observed by Doppler-free frequency-modulation spectroscopy in a standard saturated-absorption experiment using the optical arrangement shown in Fig. 1. Full details of the experimental method and sample spectra that illustrate the high signal-to-noise ratio obtained by this technique are given in Ref. 11. The same apparatus and iodine cell were used for this work.

As a check on the consistency of our results, we have used two different iodine lines for the laser stabilization. Component *t* of the transition *R*41 (6–5), whose wave number is 15379.221566 (25) cm<sup>-1</sup>, was used for approximately three quarters of the spectra. Component *i* of the transition *R*73 (5–5), whose wave number is 15233.367441 (24) cm<sup>-1</sup>, was used for the remaining spectra. Wave numbers for the iodine lines were taken from Ref. 11 and are reported with uncertainties representing a 95% confidence interval. The wave numbers used in calibrating the FT spectra were corrected to compensate for the 72-MHz frequency offset introduced in the saturating beam by the acousto-optic modulator. By stabilizing the dye laser to these iodine lines, both reference lines for our FT spectra are known at the level of better than 2 parts in 10<sup>9</sup>.

### B. Mercury-Discharge Lamps

The spectrum of neutral Hg was observed in electrodeless-discharge lamps. Eight sealed lamps were constructed of fused quartz for this experiment. Each was filled with a few mg of isotopically pure <sup>198</sup>Hg and Ar carrier gas. Two lamps each were made with Ar pressures of 33 Pa (0.25 Torr), 400 Pa (3.0 Torr), 930 Pa (7.0 Torr), and 1330 Pa (10.0 Torr). The Ar pressure in each lamp was established when the lamps were sealed off from the vacuum system on which they were prepared by using a high-precision capacitance manometer. All of the lamps were made with an inner envelope of 7-mm (inside diameter) quartz that contained the discharge surrounded by a water jacket for temperature stabilization.

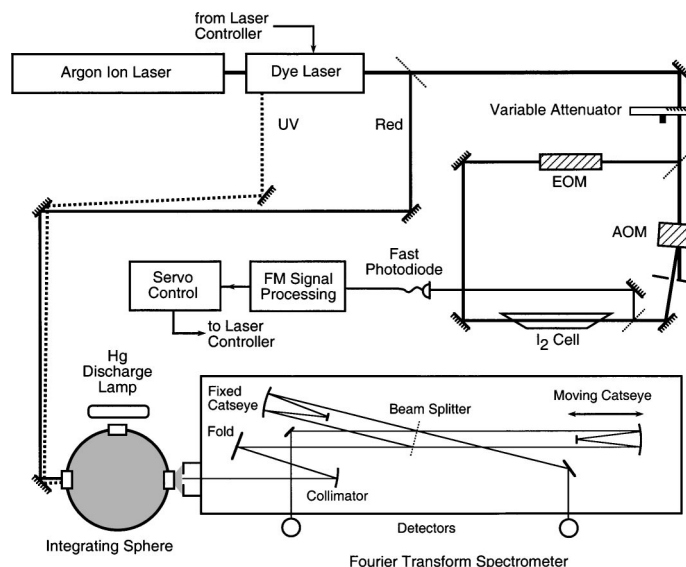


Fig. 1. Schematic representation of the experimental configuration.

The two 33-Pa lamps had an additional gas reservoir extending beyond the water jacket to provide for better long-term stability at this low Ar pressure.

The electrodeless-discharge lamps were excited by microwave radiation at 2450 MHz. For most of our spectra, power was coupled into the lamp by an Evenson-type cavity.<sup>12</sup> A few spectra were made using a cylindrical cavity. The Evenson cavity provides more efficient coupling with lower reflected power; however, its tuning is very critical, and it is easier to obtain stable long-term operation with the cylindrical cavity. Microwave power delivered to the discharge varied considerably from spectrum to spectrum but typically ranged from 20 W to 40 W.

In operation, the lamps were cooled to a temperature of 8 °C by coolant circulated through the water jacket in order to replicate the conditions of Ref. 10. In our initial experiments, water was used as the coolant; however, its strong microwave absorption made it difficult to maintain a discharge filling the entire volume of the lamp. This problem was particularly severe for the 33-Pa lamps. In addition, tuning the cavity to optimize the discharge resulted in reflected power levels exceeding 50%.

In an attempt to solve this problem, we experimented with other coolants. A solution of ethylene glycol mixed with ethanol to obtain suitable viscosity was used for a few spectra but proved to be no better than water. Most of our spectra were recorded using the silicone-based coolants HT-20 or HT-30.<sup>13</sup> These coolants were very satisfactory for the microwave excitation, absorbing little energy and permitting the cavity to be tuned for very low reflected power. Unfortunately, they were degraded by the strong UV radiation emitted by the Hg discharge causing a gradual buildup of a brown sludge in the water jacket. It was therefore necessary to clean the lamps and replace the coolant frequently to maintain adequate optical transmission.

### C. Fourier-Transform Spectrometer

The instrument used was a Chelsea Instruments FT-500,<sup>13</sup> serial number 2 of a total of four produced in the late 1980s. The design and operating characteristics have been described elsewhere.<sup>9,14</sup> The maximum optical path difference yields a limiting resolution of 0.025  $\text{cm}^{-1}$ . At the low wavelength limit of  $\sim 200$  nm, the desk-sized instrument achieves a resolving power of  $2 \times 10^6$ .

Although we used a variety of instrumental settings in the course of acquiring the data discussed here, our typical resolution was 0.03  $\text{cm}^{-1}$ , with a free spectral range of 0  $\text{cm}^{-1}$  to 39 495  $\text{cm}^{-1}$ . In order to reach the high wavenumber limit, it is necessary to sample the interferogram at position increments of the moving arm that are submultiples of the fringe crossings provided by the 15 798.01- $\text{cm}^{-1}$  control laser. Using an effective fringe division ratio of 5/2 (five samples taken per two zero crossings of the fringes of the He-Ne control laser) provided the desired range. At this spacing, 2 633 002 interferogram data points were acquired over the 16.667-cm displacement of the moving mirror corresponding to our typical resolution. A carriage velocity of 0.747 mm/s provided a data acquisition rate of 35 403  $\text{s}^{-1}$ , producing a single-scan interferogram in under 4 minutes.

The beam shear in the interferometer was adjusted daily by visual and electronic optimization of fringes from the internal-system mercury lamp (or one of the mercury lamps under test) using motorized micrometers on the cat's-eye retroreflector in the stationary arm of the interferometer. Following the daily shear adjustment, the position of zero optical path difference (ZPD) was determined as the location of the centerburst in the interferogram of a deuterium lamp built into the interferometer entry optics. Due to the broadband continuum emitted by this lamp, the interferogram is essentially zero except at a few points in the vicinity of ZPD, with a maximum in the absolute value at the data point closest to the actual zero-path position. The position of ZPD was stable throughout the day as long as the instrument was in active feedback on the fringes of the control laser.

The sensitivity of the FTS was suppressed in the region of the 632.8-nm control laser by use of blocking filters in the detector housings and photomultiplier tubes whose sensitivity decreases rapidly at wavelengths longer than 500 nm. Without these measures, desired light from the sources, attenuated by the integrating sphere, was swamped by scattered light from the control laser in the complementary optical path of the interferometer. For the present work, the signal-to-noise ratio of the normally strong 546.1-nm mercury line was degraded by this necessary loss of sensitivity at longer wavelengths.

In initial experiments with the red fundamental laser and its UV second-harmonic introduced via the integrating sphere, we found that the lasers could be useful for alignment as well as for calibration. Because the spectral bandwidth of the laser lines was significantly less than the theoretical resolution of the FTS, the native FTS instrument function (the sinc function for unapodized data) dominated the line shape in the spectrum of both lines (see Fig. 2). The degree of symmetry of the laser lines could be easily evaluated by observing the depth of the negative lobes, especially the principal negative lobe on each side of the line. This visual symmetry, especially sensitive for the UV line, was used extensively as a diagnostic for evaluating the alignment of the instrument, and was later used for the vetting of the data files (see Section 4).

Over the course of numerous experiments, we learned that several aspects of the instrument alignment were more sensitive than we had at first appreciated. Ultimately, alignment to a symmetric line shape for the unresolved UV laser line required that (1) the collimator be well focused,<sup>15</sup> (2) the beam be launched into the interferometer coaxially with the travel of the moving cat's eye,<sup>16</sup> and (3) the beam be located in space so as not to be partially occluded by the frames of the cat's eyes at any path difference. Though simple in principle, these criteria were challenging to achieve with the required degree of precision. In the course of our efforts to obtain an optimal instrumental line shape, we undertook a bottom-up reconstruction and alignment of the FTS, installing new optical mounts with improved controls for the entry optics, disassembling and reassembling the moving-arm mechanism and motor in order to replace the bearings, and adding a microscope with a video imaging system to

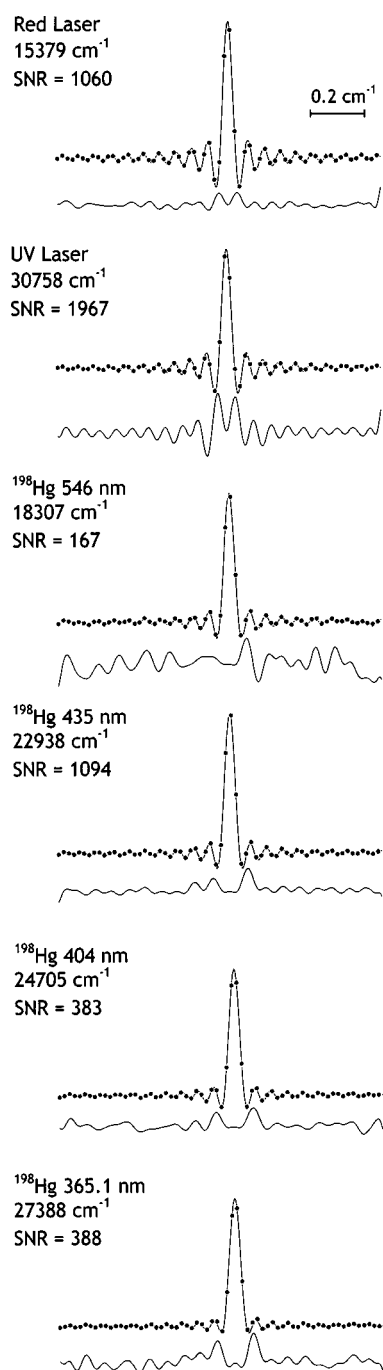


Fig. 2. Graphical summary of a single spectrum for a  $^{198}\text{Hg}$  electrodeless-discharge lamp. The solid circles represent the transform of the experimental interferogram zero filled to  $2^{22}$  data points. The solid curve through these points is the fitted profile. The residuals to the fit are shown vertically displaced and magnified by a factor of 10. The fit and the residuals are calculated from a fourfold Fourier interpolated spectral segment, as described in the text.

observe the interference fringes at low light levels and high magnification.

### 3. DATA ANALYSIS

#### A. Transformation and Fitting

Experimental interferograms and spectra were processed using GREMLIN, a software package developed by James

Brault as a further development of his earlier program DECOMP.<sup>17</sup> The 2.63-million-point experimental interferogram was first symmetrized about the experimentally determined ZPD point by truncating the side with the greater number of data points.<sup>18</sup> The resulting data were then zero filled symmetrically to give a double-sided interferogram whose length corresponded to a power of 2 as required for the fast-Fourier-transform algorithm, in this case 4 194 304 or  $2^{22}$  data points.

Phase correction of the data was accomplished interactively following the procedure described by Learner *et al.*<sup>18</sup> The correction was typically stable throughout an operating day, indicating the absence of major changes in alignment or the loss of tracking of control laser fringes by the system.

The transform of the interferogram yielded a complex spectrum with data spacing of  $0.0188\text{ cm}^{-1}$  per point over the free spectral range from  $0\text{ cm}^{-1}$  to  $39\,495\text{ cm}^{-1}$ . The increase in data density over the  $0.03\text{-cm}^{-1}$  resolution is in direct proportion to the fractional zero filling of the interferogram. Thus the instrument-limited laser line profiles were represented by three to four data points between the first zero crossings of the sinc function instead of two. Further spectral manipulations were performed on the real part only.

A program was written in C++ to measure the spectra by fitting the line profiles using a nonlinear least-squares analysis. A  $1.2\text{-cm}^{-1}$  segment of the spectrum was extracted around each of the two laser lines and four Hg lines. These data were interpolated by a factor of 4 prior to fitting. For the analysis, we used a sinc function as an appropriate approximation to the FTS instrumental line shape. The actual instrumental line shape is shifted and slightly broadened by amounts proportional to the wave number owing to the finite aperture of the instrument.<sup>16,19</sup> This broadening is symmetric about the shifted center of the profile, and the relative positions of the zero crossings with respect to the center are unchanged. For our instrument with a 1-mm aperture, the actual instrumental line shape does not differ by more than 0.8% of its maximum value from a simple sinc. Since the laser lines have negligible spectral width with respect to the instrumental width, they were fitted to the sinc function. The mercury lines were fitted to the convolution of a Voigt function with a sinc function. The wave numbers for each line determined in these fits represent the uncorrected scale of the spectrum, with the two laser lines to be used as calibrants for the four mercury lines.

#### B. Managing the Population of Spectra

Each spectrum was summarized graphically, as shown in Fig. 2, permitting careful visual inspection of the line shapes. Inspection was facilitated by the display of the interpolated spectrum, the fitted profile, and most important, the residuals of the fit. Examination of the residuals is a very sensitive measure of line asymmetry. Spectra that exhibited anomalous asymmetry for the laser lines were rejected from our composite results. Of the 126 spectra acquired, 19 were rejected.

## 4. RESULTS AND DISCUSSION

### A. Laser-Line Calibration

The ratio of the fitted position for the UV laser line to the fitted position for the red laser line was calculated for each of the 107 spectra retained for the  $^{198}\text{Hg}$  measurements. The frequency distribution of this ratio about the expected value of 2.0 is shown in Fig. 3(a), and the underlying data are shown in run order in Fig. 3(b). Close examination of Fig. 3(b) reveals that the distribution of the ratios is not entirely random in time but shows some correlation with run order. This suggests that the deviation of the ratio from 2.0 may be associated with instrument alignment factors that drift slightly with time.

Values for the calibration factor  $k_{\text{eff}}$  were computed from each of the laser lines as

$$k_{\text{eff}} = (\sigma_{\text{true}}/\sigma_{\text{apparent}}) - 1.$$

For each spectrum, we averaged the values of  $k_{\text{eff}}$  provided by the two laser lines and used this average correction factor to calibrate the spectrum. The relative mean bias of  $6.1 \times 10^{-9}$  calculated from the data in Fig. 3 was taken as an indicator of the limiting accuracy of the instrument. Each line position was therefore assigned an uncertainty component of  $6.1 \times 10^{-9}$  times the central wave number of the line.

### B. $^{198}\text{Hg}$ Measurements

The results for the four lines of  $^{198}\text{Hg}$  measured in this work are given in Table 1. For each line we present the measured wave number at each of four Ar buffer-gas pressures studied. The number of observations was 41, 36, 7, and 21 for the 33-Pa, 400-Pa, 930-Pa, and 1330-Pa lamps, respectively. For each Ar pressure, the measurements were divided approximately equally between the two Hg lamps. In no instance was there any statistically significant difference between the wave numbers measured in the two lamps. The two different iodine lines used for laser stabilization also gave results that were statistically indistinguishable. The wave numbers we report are the simple means of all measurements with the exception of those from the few spectra that were discarded entirely on the basis of poor laser-line profiles as described above.

The relative uncertainty of each result in Table 1 is calculated as the quadrature sum of the relative standard deviation of the mean, the relative uncertainty of the calibration laser wave number (approximately  $8.5 \times 10^{-10}$ ), the relative uncertainty due to the uncertainty of the Ar pressure in the lamp (estimated to be 1.3 Pa), and an estimated nonstatistical relative uncertainty of  $6.1 \times 10^{-9}$  in the determination of the multiplicative correction (1

+  $k_{\text{eff}}$ ). The uncertainties are dominated by this fourth contribution, which is included to reflect the fact that, when averaged over all of our spectra, the UV and red laser wave numbers are not found to be in an exact ratio of

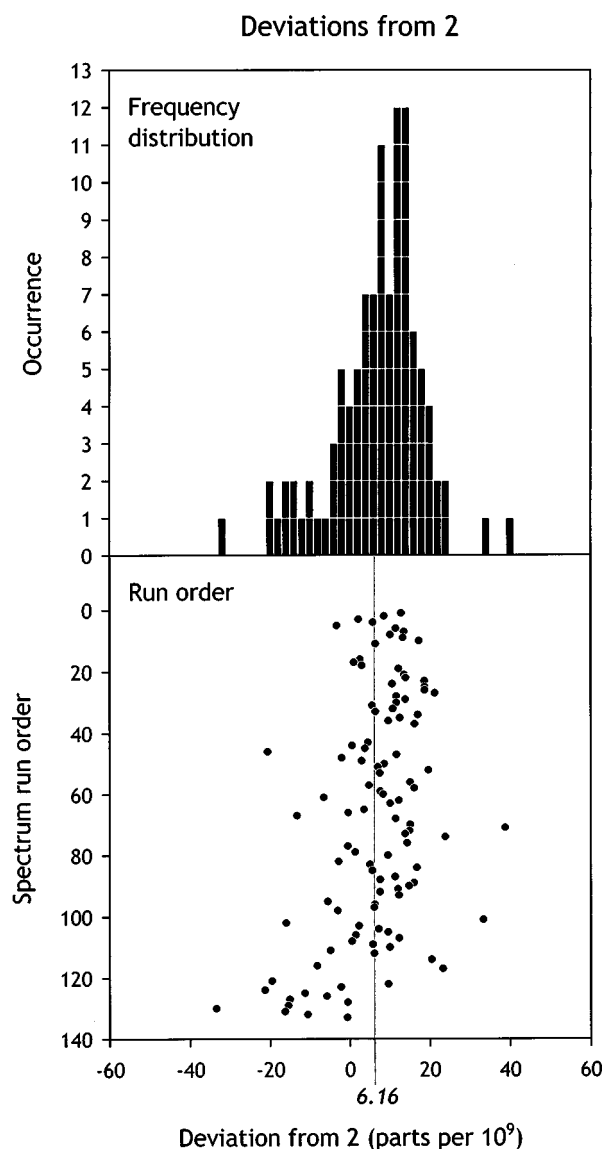


Fig. 3. Distribution of the observed deviation of the ratio of the UV to visible laser frequencies from the expected value of 2.0. (a) Frequency-distribution histogram for all 107 spectra. (b) Distribution of deviations by run order. The mean relative deviation of  $6.16 \times 10^{-9}$  is taken to be the limiting relative accuracy of this method of measuring wavelengths.

**Table 1. Measured Wave Numbers for Prominent Lines of  $^{198}\text{Hg}$  at Various Ar Carrier Gas Pressures<sup>a</sup>**

Pressure (Pa)	Hg Line			
	546.1 nm	435.8 nm	404.7 nm	365.0 nm
33	18307.40481(24)	22938.08202(29)	24705.29887(31)	27388.27973(34)
400	.40413(23)	.08113(29)	.29806(31)	.27936(34)
930	.40301(24)	.08011(29)	.29701(31)	.27835(35)
1330	.40248(24)	.07944(29)	.29635(31)	.27752(35)

<sup>a</sup>Uncertainties are given at a 95% level of confidence. Hg wave numbers are in  $\text{cm}^{-1}$ .

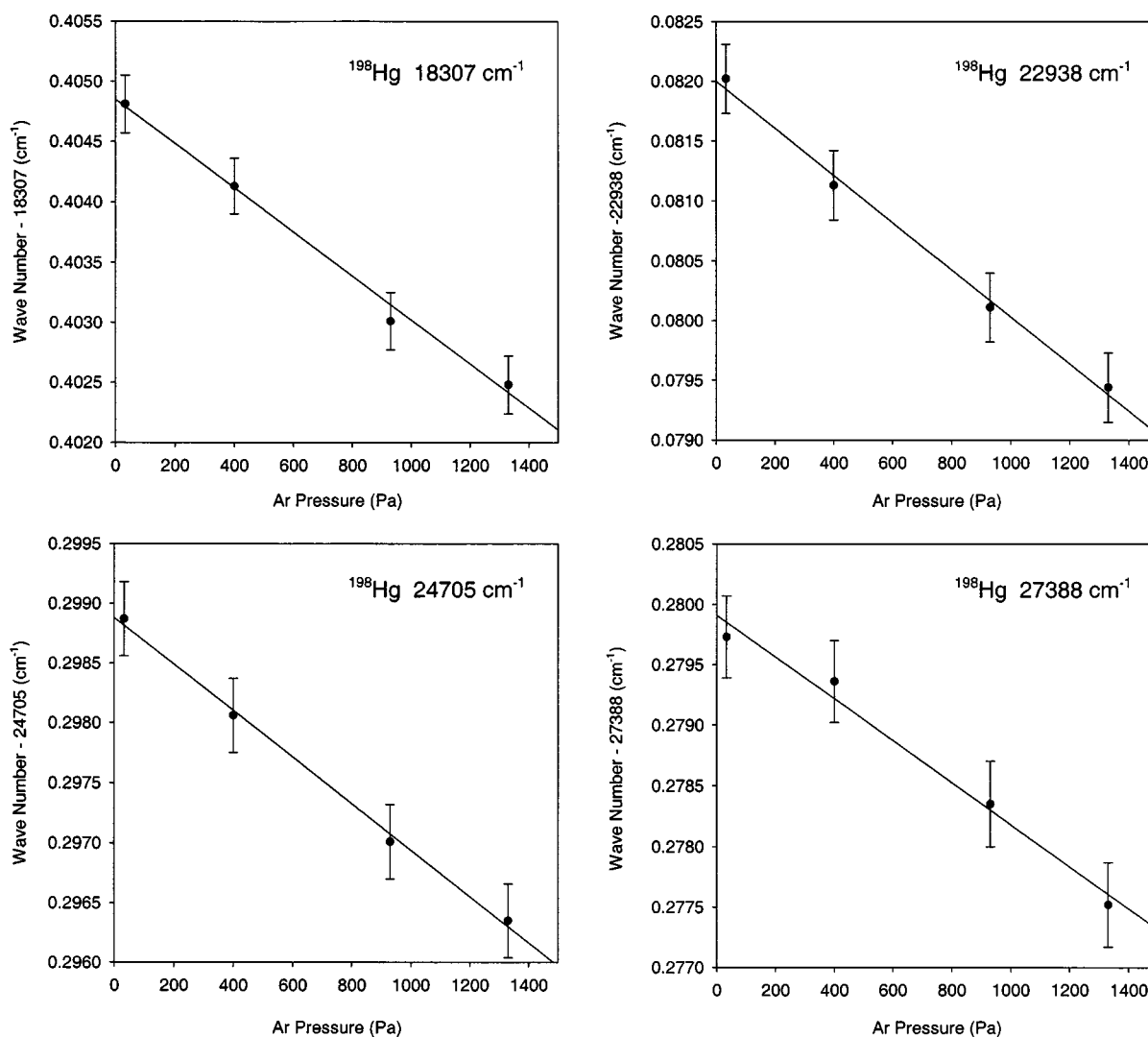


Fig. 4. Ar-pressure dependence of  $^{198}\text{Hg}$  wave numbers observed in our measurements. Error bars are one standard deviation.

2.0. The uncertainties presented in Table 1 have been expanded by a factor of 2 to provide a 95% confidence level.

The Ar-pressure dependence of the Hg wave numbers is illustrated in Fig. 4. For all four lines, the pressure dependence is well defined and linear. Ar-pressure-shift rates and zero-pressure wave numbers for each line were determined by making a weighted linear least-squares fit to the data. These results are given in Table 2. To the accuracy of our measurements, there is no statistically significant difference in the shift rates for these four lines. From the pressure-shift results in Table 2, it is possible to calculate the wave numbers for these Hg lines at any desired pressure with uncertainties comparable to the measurement uncertainty. In Table 3, we display the calculated wave numbers and their deviations from the measured values at the four pressures studied in this work.

Our results are compared with the Fabry-Perot measurements of Kaufman<sup>10</sup> in Fig. 5. The uncertainty of the measurements in Ref. 10 is estimated to be 0.0001 Å. For purposes of comparison, we assume this estimate to

represent a 95% confidence interval. Our results are in excellent agreement with Kaufman for the 1330-Pa lamp. At lower Ar pressures, the results of Ref. 10 have a slight bias to higher wave number, especially for the 33-Pa lamp. As a consequence, the Ar shift rates given by Kaufman are higher than our determinations (Table 1) by a factor of 1.25 to 1.5.

**Table 2. Ar-Pressure-Shift Rates and Zero-Pressure Wave Numbers for Prominent Lines of  $^{198}\text{Hg}^a$**

Zero-Pressure Wave Number (cm $^{-1}$ )	Ar-Pressure-Shift Rate (cm $^{-1}$ /Pa) $\times 10^6$
18307.40485 (20)	-1.83 (24)
22938.08200 (24)	-1.97 (29)
24705.29888 (26)	-1.94 (31)
27388.27991 (29)	-1.73 (34)

<sup>a</sup>Uncertainties are given at a 95% level of confidence.

### C. Reexamination of Prior Results

Based on the wave numbers and pressure-shift rates determined in this work, we have reexamined the results of Ref. 9 that suggested a linear dependence of the value of  $k_{\text{eff}}$  on wave number. For this purpose, we made new observations of the lamp that was used in the earlier work. This lamp had a nominal pressure of 400 Pa. For the new observations, we calculated  $k_{\text{eff}}$  using as standards both the 400-Pa wave numbers from our current work and those of Kaufman.<sup>9</sup> The results are shown in Fig. 6. When the standards are taken from Kaufman, the results suggest a trend of increasing  $k_{\text{eff}}$  with increasing wave number similar to that observed in Ref. 9. Our new spectra do not extend to wavelengths as short as those recorded in the earlier work; however, a reexamination of the old data shows that all lines in both the new and old spectra are consistent with a slope of  $2.4(6) \times 10^{-12}$  per  $\text{cm}^{-1}$  in  $k_{\text{eff}}$ . When values of  $k_{\text{eff}}$  are calculated using as standards our present results, on the other hand, there is no evidence of a wave-number dependence. We conclude that the apparent dependence of  $k_{\text{eff}}$  on wave number observed in Ref. 9 for the 400-Pa lamp can be attributed to small inaccuracies in the results of Kaufman.

However, the value of  $k_{\text{eff}}$  determined by taking as standards the 400-Pa results of our current work is in serious disagreement with the value calculated from the calibration lasers. This disagreement encouraged us to explore the possibility that the pressure in the lamp was not actually 400 Pa. Unlike the new lamps made for the present work, the old lamp was not fabricated using a capacitance manometer to determine the Ar pressure.

To estimate the Ar pressure in the lamp, we corrected the observed Hg wave numbers using for  $k_{\text{eff}}$  the average of the values calculated for the red and UV lasers. The corrected wave numbers were combined with the Ar pressure-shift results from Table 2 to calculate a value of the Ar pressure in the lamp for each of the four Hg lines. The results were reasonably consistent, producing a value of  $670 \text{ Pa} \pm 33 \text{ Pa}$  ( $5.0 \text{ Torr} \pm 0.25 \text{ Torr}$ ) for the lamp pressure. Assuming this to be the correct pressure for the lamp, we calculated the Hg wave numbers at a pressure of 670 Pa and used these values as standards to calculate  $k_{\text{eff}}$ . The result, shown in Fig. 6, is consistent with the laser results and has no statistically significant dependence on wave number. These results demonstrate that obtaining values of  $k_{\text{eff}}$  that show no significant dependence on wave number is not a sufficient test to en-

sure that the derived value of  $k_{\text{eff}}$  is correct. If wavelengths of  $^{198}\text{Hg}$  are to be used as standards for calibration of spectra from an FTS, accurate knowledge of the Ar pressure in the Hg lamp is essential.

## 5. CONCLUSIONS

The fundamental and second-harmonic beams of a frequency-stabilized laser have been used to investigate basic issues concerning the calibration and ultimate measurement accuracy of a high-resolution FTS. The ratio of the measured line centers for laser lines known to exhibit an energy ratio of exactly 2.0 was found to vary by as much as one or two parts in  $10^8$  for individual spectra. The average calibration bias for our ensemble of 107 independent spectra was approximately 6 parts in  $10^9$ . This establishes a lower limit on the relative calibration accuracy that can be expected for our instrument. Our ability to obtain and maintain optimal alignment of the FTS appears to be a limiting factor in the uncertainty of the wave-number scale.

High-resolution spectra of four intense lines from  $^{198}\text{Hg}$  electrodeless discharge lamps combined in an integrating sphere with the calibration radiation from the fundamental and second-harmonic beams of the frequency-locked

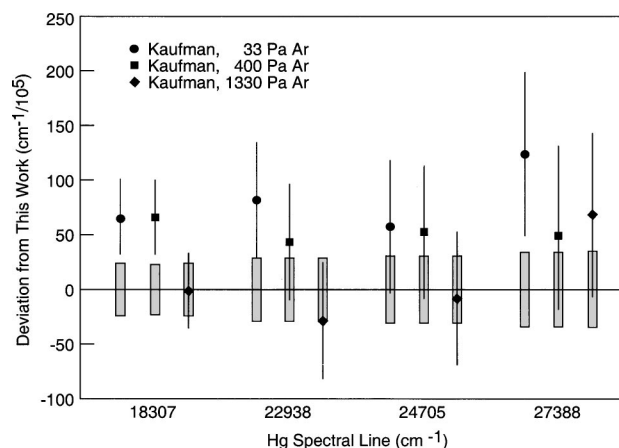


Fig. 5. Comparison of our results with the  $^{198}\text{Hg}$  wave numbers reported by Kaufman.<sup>10</sup> The data are presented as deviations from this work with uncertainties shown at a 95% confidence interval. Uncertainties for this work are represented as gray bars centered about zero.

**Table 3. Wave Numbers of Prominent Lines of  $^{198}\text{Hg}$  at Various Ar Pressures Calculated from the Pressure-Shift Results in Table 2 ( $\sigma_{\text{calc}}$ ) and Deviations from the Measured Values ( $\Delta$ )<sup>a</sup>**

Argon Pressure (Pa)	Hg Wave Number ( $\text{cm}^{-1}$ )							
	18307		22938		24705		27388	
	$\sigma_{\text{calc}}$	$\Delta^a$	$\sigma_{\text{calc}}$	$\Delta^a$	$\sigma_{\text{calc}}$	$\Delta^a$	$\sigma_{\text{calc}}$	$\Delta^a$
33	.40478(20)	3	.08194(24)	8	.29881(26)	6	.27985(28)	12
400	.40411(22)	2	.08121(26)	8	.29810(28)	4	.27922(32)	14
930	.40313(30)	12	.08016(36)	5	.29707(40)	6	.27829(44)	6
1330	.40240(38)	8	.07937(29)	7	.29629(50)	6	.27760(54)	8

<sup>a</sup>Uncertainties are given at a 95% level of confidence.

<sup>b</sup> $\Delta = (\sigma_{\text{calc}} - \sigma_{\text{meas}}) \times 10^5$ .

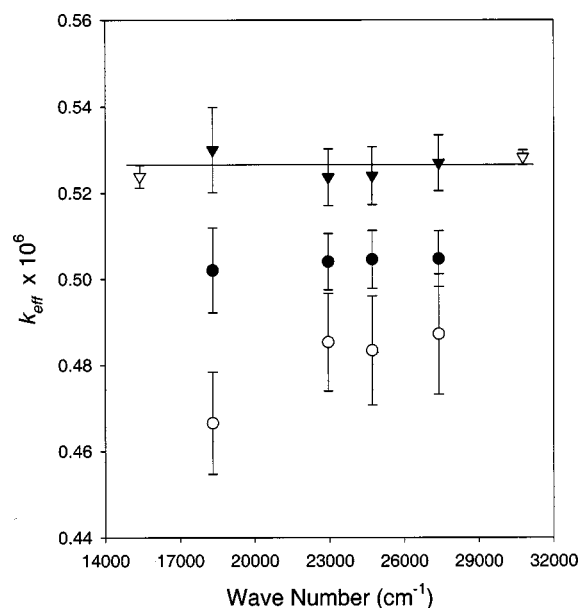


Fig. 6. Values of the correction factor  $k_{\text{eff}}$  calculated for spectra acquired using the same  $^{198}\text{Hg}$  lamp observed in Ref. 9. Open circles represent  $k_{\text{eff}}$  based on the 400-Pa results of Kaufman,<sup>10</sup> solid circles represent  $k_{\text{eff}}$  based on the 400-Pa results of this work, and filled triangles represent  $k_{\text{eff}}$  based on  $^{198}\text{Hg}$  wave numbers calculated using the pressure-shift results of this work for an assumed Ar pressure of 670 Pa. Open triangles represent  $k_{\text{eff}}$  calculated from the red and UV calibration lasers. In this figure, the error bars represent random variation at the one standard deviation level. The horizontal line represents the average of the two laser values, which is regarded as the most reliable determination of the true value of  $k_{\text{eff}}$ .

laser have been obtained using a carefully aligned Fourier-transform spectrometer. The internal check on the consistency of the results provided by the two laser lines sets a floor on the accuracy we can expect in the  $^{198}\text{Hg}$  measurements. On the basis of a statistical treatment alone, we would have estimated the uncertainties to be much smaller. Nevertheless, our new measurements represent a significant improvement on the previously reported values.<sup>10</sup>

Our new wave numbers and pressure-shift coefficients for four lines in  $^{198}\text{Hg}$  are sufficiently accurate that these lines may be used to calibrate a spectrum acquired with an FTS without need for the frequency-locked laser system. In fact, we have used the same Hg electrodeless-discharge lamps observed in this experiment to acquire internally calibrated spectra for the measurement of wave numbers and pressure shifts for weaker lines of Hg and Ar. These results will be published separately. The lines are also sufficiently intense to be used with an integrating sphere as external calibrants.

In earlier work<sup>9</sup> using for calibration the  $^{198}\text{Hg}$  results of Kaufman,<sup>10</sup> we found evidence of a monotonic variation in the correction factor  $k_{\text{eff}}$  as a function of wave number. Our present observations, using for calibration the fundamental and second harmonic of a laser, show no statistically significant evidence of wave-number dependence in  $k_{\text{eff}}$ . We conclude that the adequacy of a single multiplicative correction factor for the absolute calibration of an individual FT spectrum is supported by our data at the level of better than a part in  $10^8$ . This property of FTS

permits the propagation of high-accuracy laser-spectroscopic measurements of isolated line positions to a broadband coverage of atomic wavelengths in emission spectra.

\*Permanent address: Department of Physics, University of Zagreb, Zagreb, Croatia.

## REFERENCES AND NOTES

- G. Horlick and W. K. Yuen, "Atomic spectrochemical measurements with a Fourier transform spectrometer," *Anal. Chem.* **47**, 775A–781A (1975).
- P. Luc and S. Gerstenkorn, "Fourier transform spectroscopy in the visible and ultraviolet range," *Appl. Opt.* **17**, 1327–1331 (1978).
- J. W. Brault, "Fourier transform spectrometry in relation to other passive spectrometers," *Philos. Trans. R. Soc. London, Ser. A* **307**, 503–511 (1982).
- L. M. Faires, "Fourier transforms for analytical atomic spectroscopy," *Anal. Chem.* **58**, 1023A–1034A (1986).
- A. Thorne, "High-resolution Fourier transform atomic spectrometry," *J. Anal. At. Spectrom.* **2**, 227–232 (1987).
- A. P. Thorne, "Fourier transform spectrometry in the ultraviolet," *Anal. Chem.* **63**, 57A–65A (1991).
- R. C. M. Learner and A. P. Thorne, "Wavelength calibration of Fourier-transform emission spectra with applications to Fe I," *J. Opt. Soc. Am. B* **5**, 2045–2059 (1988).
- A. P. Thorne and R. C. M. Learner, "High resolution FTS of atoms and molecules in the ultra-violet," *Mikrochim. Acta* **II**, 445–448 (1988).
- M. L. Salit, J. C. Travis, and M. R. Winchester, "Practical wavelength calibration considerations for UV-visible Fourier-transform spectroscopy," *Appl. Opt.* **35**, 2960–2970 (1996).
- V. Kaufman, "Wavelengths, energy levels, and pressure shifts in mercury 198," *J. Opt. Soc. Am.* **52**, 866–870 (1962).
- C. J. Sansonetti, "Precise measurements of hyperfine components in the spectrum of molecular iodine," *J. Opt. Soc. Am. B* **14**, 1913–1920 (1997).
- F. C. Fehsenfeld, K. M. Evenson, and H. P. Broida, "Microwave discharge cavities operating at 2450 MHz," *Rev. Sci. Instrum.* **36**, 294–298 (1963).
- To describe experimental procedures adequately, it is occasionally necessary to identify commercial products by manufacturer. In no instance does such identification imply endorsement by the National Institute of Standards and Technology, nor does it imply that the particular products or equipment are necessarily the best available for the purpose.
- A. P. Thorne, C. J. Harris, I. Wynne-Jones, R. C. M. Learner, and G. Cox, "A Fourier transform spectrometer for the ultraviolet: design and performance," *J. Phys. E* **20**, 54–60 (1987).
- P. Saarinen and J. Kauppinen, "Spectral line-shape distortions in Michelson interferometers due to off-focus radiation source," *Appl. Opt.* **31**, 2353–2359 (1992).
- J. Kauppinen and P. Saarinen, "Line-shape distortions in misaligned cube corner interferometers," *Appl. Opt.* **31**, 69–74 (1992).
- J. W. Brault and M. C. Abrams, "DECOMP: a Fourier transform spectra decomposition program," *High Resolution Fourier Transform Spectroscopy*, Vol. 6 of 1989 Technical Digest Series (Optical Society of America, Washington, D.C., 1989), pp. 118–121.
- R. C. M. Learner, A. P. Thorne, I. Wynne-Jones, J. W. Brault, and M. C. Abrams, "Phase correction of emission line Fourier transform spectra," *J. Opt. Soc. Am. A* **12**, 2165–2171 (1995).
- J. Genest and P. Tremblay, "Instrument line shape of Fourier transform spectrometers: analytic solutions for non-uniformly illuminated off-axis detectors," *Appl. Opt.* **38**, 5438–5446 (1999).